Excess Centrosomes Disrupt Vascular Lumenization and Endothelial Cell Adherens Junctions

Danielle B Buglak[a], Erich J Kushner[b], Allison P Marvin[b], Katy L Davis[b], and Victoria L Bautch[a,b,c,#]

[a]Curriculum in Cell Biology and Physiology, The University of North Carolina at Chapel Hill, Chapel Hill, North Carolina 27599, USA.
[b]Department of Biology, The University of North Carolina at Chapel Hill, Chapel Hill, North Carolina 27599, USA.
[c]McAllister Heart Institute, The University of North Carolina at Chapel Hill, Chapel Hill, North Carolina 27599, USA.

[#]Corresponding author: Victoria L Bautch, PhD
Professor of Biology
Department of Biology, CB#3280
University of North Carolina at Chapel Hill
Chapel Hill, NC 27599 USA
Phone: 919-966-6797
E-mail: bautch@med.unc.edu

Running head: CENTROSOMES IN VASCULAR LUMENIZATION AND JUNCTIONS

WORKING TITLE: 10 words
Abstract: 145 words
Text: 5,181 words
Figures: 4 main, 3 supplemental

ABSTRACT

Proper blood vessel formation requires coordinated changes in endothelial cell polarity and rearrangement of cell-cell junctions to form a functional lumen. One important regulator of cell polarity is the centrosome, which acts as a microtubule organizing center. Excess centrosomes perturb aspects of endothelial cell polarity linked to migration, but whether centrosome number influences apical-basal polarity and cell-cell junctions is unknown. Here, we show that excess centrosomes alter the apical-basal polarity of endothelial cells in angiogenic sprouts and disrupt endothelial cell-cell adherens junctions. Endothelial cells with excess centrosomes had narrower lumens in a 3D sprouting angiogenesis model, and zebrafish intersegmental vessels had reduced perfusion following centrosome overduplication. These results indicate that endothelial cell centrosome number regulates proper lumenization downstream of effects on apical-basal polarity and cell-cell junctions. Endothelial cells with excess centrosomes are prevalent in tumor vessels, suggesting how centrosomes may contribute to tumor vessel dysfunction.

Keywords: Endothelial cell, centrosome, junctions, polarity, lumen, angiogenesis

INTRODUCTION

Angiogenesis is the sprouting of new blood vessels from pre-existing vessels and is crucial during development, pregnancy, wound healing, and tumorigenesis [1–3]. Endothelial cells (EC) form new sprouts to provide conduits for blood flow and create a functional vascular network. This process requires dynamic rearrangement of endothelial cell-cell junctions and establishment of apical-basal polarity [4–8]. Lumenization closely follows sprout formation and extension temporally, and many sprout tips have multiple EC that are polarized in the apical-basal axis [9]. However, it is not known how centrosome number contributes to this process.

As tumors grow, hypoxia leads to elevated levels of pro-angiogenic factors that promote neo-angiogenesis to vascularize the tumor. However, the blood vessels surrounding these tumors are often leaky, tortuous, and not properly lumenized [10–12], suggesting defects in EC junctions and polarity. Interestingly, tumor vessels are also characterized by EC with excess centrosomes [13,14]. The centrosome acts as a major microtubule organizing center and determinant of cell polarity [15,16]. High VEGF-A signaling in EC results in centrosome overduplication, which affects interphase cells by increasing invasiveness, elevating microtubule nucleations, changing aspects of polarity and migration, and altering signaling dynamics [13,17–19]. However, it is unclear how excess centrosomes impact cell-cell interactions and lumenogenesis.

Cadherins form cell-cell adherens junctions that link to the actin cytoskeleton and restrict the apical vs. basolateral domains [20,21]. In EC, VE-cadherin is the primary

89 component of the vascular adherens junction and is required for localization of apical
90 markers during lumen formation in zebrafish [7]. Depletion of VE-cadherin is
91 embryonically lethal in zebrafish and mice due to severe vascular defects, including a
92 lack of vascular lumens [22,23]. However, the effects of centrosome number on
93 adherens junctions have not been investigated.
94
95 Here, we show for the first time that excess centrosomes prevent the proper
96 polarization of interacting EC. Excess centrosomes resulted in EC with destabilized
97 adherens junctions and narrow and closed vascular lumens both *in vitro* and *in vivo*.
98 These findings reveal a novel role for the centrosome in EC apical-basal polarity, and in
99 junction and lumen formation, and suggest how excess centrosomes in the vasculature
100 may contribute to poor perfusion in tumor vessels.

101 **RESULTS**

102 ***Excess centrosomes perturb polarization of junctionally linked EC***

103 We previously showed that excess centrosomes interfere with repolarization
104 along the forward-rearward axis in sprouting EC [17], and thus we hypothesized that
105 supernumerary centrosomes disrupt multiple EC polarity axes. We examined the
106 polarity between EC sharing junctions using an inducible system to overexpress polo-
107 like kinase 4 (Plk4) in human umbilical vein endothelial cells (HUVEC) **(Fig. 1a)**. Plk4
108 regulates centriole duplication, and its overexpression downstream of a TRE (tet-
109 responsive element) upon addition of doxycycline (DOX) results in supernumerary
110 centrosomes [13,17,24,25]. TRE-Plk4 HUVEC were seeded onto large H-shaped
111 micropatterns that allow for polarity assessment between two EC that form a cell-cell
112 junction. Polarity was defined based on centrosome position relative to the nucleus and
113 cell-cell junction, with a “proximal” position being near the cell-cell junction, a “central”
114 position in the nuclear region, and a “distal” position between the nucleus and the cell
115 periphery **(Fig. 1b)**. Two EC with a normal centrosome number (1-2) typically had a
116 distal centrosome polarity **(Fig. 1c-d)**. In contrast, two EC with excess centrosomes (>2)
117 showed a significant increase in central/proximal polarity, indicating that centrosome
118 number affects EC polarization relative to cell-cell junctions **(Fig. 1c-d)**. Interestingly,
119 when a normal EC and an EC with excess centrosomes were linked on the same
120 pattern (N:O), normal EC had a higher frequency of aberrant centrosome localization
121 than N:N counterparts, while EC with excess centrosomes had a higher frequency of
122 normal centrosome localization relative to O:O counterparts, suggesting that EC polarity
123 influences polarity in neighboring cells **(Fig. 1d)**. Furthermore, when two EC with normal

124 centrosome number (N:N) formed a junction, both cells usually had centrosomes in the
125 distal position, which we termed “distal” polarity **(Fig. 1e)**. All other polarity combinations
126 were deemed “other”. When both EC forming a junction had excess centrosomes (O:O),
127 polarity was randomized between distal and other **(Fig. 1e)**. Additionally, N:N EC
128 combinations were more likely to have cells with matching polarity, while EC with an
129 O:O combination were less likely to have the same polarity as their neighbor **(Fig. 1f).**
130 Taken together, these data indicate that excess centrosomes prevent proper EC
131 polarization relative to cell-cell junctions.
132

133 ***EC with excess centrosomes form disorganized adherens junctions***

134 Because interacting EC with excess centrosomes had perturbed polarity in the
135 junction axis, we asked whether EC cell-cell interactions were influenced by centrosome
136 number. Adherens junctions are required for proper apical-basal polarity in epithelial
137 cells [7,26], and the distribution of VE-cadherin at EC adherens junctions is indicative of
138 junction maturity; a linear VE-cadherin pattern is associated with mature stabilized
139 junctions, while a serrated and punctate VE-cadherin pattern is associated with
140 activated and/or disrupted junctions [27]. To determine how excess centrosomes
141 influence adherens junctions, we seeded induced tet-Plk4 HUVEC onto H-shaped
142 micropatterns. Due to the heterogeneous nature of Plk4-induced centrosome over-
143 duplication, a given cell-cell junction could have contributions from two EC with a normal
144 number of centrosomes (N:N), two EC with excess centrosomes (O:O), or one of each
145 (N:O) **(Fig. 2a-a”)**. We found that junctions with contributions from EC with normal
146 centrosome numbers had more linear and stable junctions, while junctions with

147 contributions from EC with excess centrosomes formed more chaotic and disrupted
148 junctions **(Fig. 2b-b", c-c")**. These chaotic junctions had increased total VE-cadherin
149 area **(Fig. 2d)**, and line scans revealed a more dispersed VE-cadherin junction
150 distribution when one or both EC had excess centrosomes **(Fig. 2e)**. We also assessed
151 the overall width of the junction and found that junctional VE-cadherin distribution was
152 wider in junctions formed when one or both EC had excess centrosomes **(Fig. 2f)**.
153 Together, these data suggest that both the junction shape and VE-cadherin distribution
154 are perturbed in EC with supernumerary centrosomes. Because tight junctions are
155 maintained along with ectopic patches of VE-cadherin in migrating and anastomosing
156 EC [28], we examined tight junctions via ZO-1 staining and found that both N:O and
157 O:O patterns had missing or abnormal tight junctions downstream of disrupted
158 adherens junctions, with O:O patterns having a more severe disruption **(Fig. S1)**. In
159 these cases, there was no organized ZO-1 staining in the large patches of VE-cadherin
160 beyond the junction site. Overall, these findings indicate that EC with excess
161 centrosomes do not maintain proper endothelial cell-cell adherens or tight junctions.
162

163 ***EC with excess centrosomes have abnormal lumens***

164 We hypothesized that the disrupted polarity seen between EC with
165 supernumerary centrosomes had physiological consequences. To further examine EC
166 polarity, we analyzed lumenized sprouts that form and polarize in the apical-basal axis
167 in a 3D sprouting angiogenesis assay [9,29]. DOX-treated tet-Plk4 HUVEC expressing
168 centrin::eGFP were stained for Moesin1 as an apical marker, since Moesin1 localizes to
169 F-actin found at apical EC cell-cell contacts [6] **(Fig. 3a-b)**. We found that EC with

170 normal centrosome numbers (1-2) typically had apically positioned centrosomes, while
171 EC with excess centrosomes (>2) had randomized centrosome polarity in the apical-
172 basal axis **(Fig. 3b-c)**. In addition, EC with excess centrosomes were more likely to
173 have punctate Moesin1, basal Moesin1, or unpolarized abnormal Moesin1 staining
174 patterns compared to normal linear and apical patterns **(Fig. 3b, d)**, indicative of polarity
175 defects. Furthermore, VE-cadherin around EC with excess centrosomes was more
176 dispersed in 3D sprouts compared to EC with normal centrosome number **(Fig. S2a)**.
177
178 Since both apical-basal polarity and proper junction formation are important for
179 lumen formation [4–8], we hypothesized that excess centrosomes in EC perturb vessel
180 lumenogenesis. After normalizing for overall vessel width, vessel lumen widths were
181 narrower near EC with excess centrosomes (excluding closed lumens) compared to EC
182 with normal centrosome numbers **(Fig. 3b, e)**, and raw lumen widths were also
183 decreased **(Fig. S2b)**. Interestingly, some lumens were completely closed around EC
184 with supernumerary centrosomes, and the incidence of closed and narrowed lumens
185 was elevated near sprout EC with excess centrosomes **(Fig. 3f)**. These findings indicate
186 that EC centrosome number regulates proper vessel lumen diameter, likely through
187 effects on apical-basal polarity.
188
189 ***Overexpression of Plk4 in zebrafish results in fewer lumenized vessels***
190 To determine if centrosome number affects lumen formation *in vivo*, we utilized a
191 zebrafish model with vascular-specific Cre-mediated overexpression of *Plk4* **(Fig. S3a)**,
192 and crossed to *Tg(fli:centrin-GFP)* fish to visualize EC centrosomes. Fish

193 overexpressing *Plk4* had increased EC with >2 centrosomes **(Fig. S3b-c)**, and
194 microangiography at 72 hpf revealed that these fish also had fewer perfused
195 intersegmental vessels (ISVs) compared to wild type controls or fish lacking Cre **(Fig.**
196 **4a-b)**. Lumens of perfused vessels in fish with *Plk4* overexpression were narrower
197 compared to controls, and more lumens were completely closed or narrowed **(Fig. 4c-**
198 **d)**. To further test the effects of supernumerary centrosomes, we generated a second
199 zebrafish model by utilizing the *Gal4-UAS* system to transiently overexpress *Plk4* in
200 blood vessels **(Fig. S3d)**. ISVs containing EC with excess centrosomes were narrower
201 than neighboring ISVs consisting of EC with 1-2 centrosomes, and ISVs from fish
202 lacking *Tg(fli:Gal4)* **(Fig. 4e-f)**. These findings indicate that ISV narrowing is specific to
203 sprout regions with EC harboring excess centrosomes. Reduced vessel perfusion,
204 coupled with narrow or blocked lumens and vessels, suggests that excess centrosomes
205 in EC lead to disrupted lumenogenesis *in vivo*.

206 **DISCUSSION**

207 Angiogenesis involves migration and rearrangement of EC, and leads to new
208 conduits through anastomosis and lumen formation between adjacent EC [1–3]. Cell-
209 cell interactions and polarization in several axes are important for lumen formation, but
210 the role of the centrosome in these processes is poorly understood. Here, we show that
211 supernumerary centrosomes perturb EC polarity and cell adhesion and disturb lumen
212 formation *in vitro* and *in vivo*, implying that the centrosome is involved in both junctional
213 adhesion and the apical-basal polarization that precedes vascular lumen formation or
214 stabilization.

215

216 Our data highlights important roles for the centrosome in maintaining junction
217 integrity and lumen development in interphase cells. Besides overduplication,
218 centrosome function is impacted by centriole loss or structural defects. Mis-localization
219 of centrosomal proteins, structural deficits, and centrosome loss all result in G1 cell-
220 cycle arrest [30], and compromise analysis of effects of centrosome loss on interphase
221 cell behavior. Although supernumerary centrosomes affect cellular processes, they do
222 not acutely block cell-cycle progression [17] and thus allow for analysis of centrosome
223 perturbation on interphase behaviors.

224

225 Our previous work showed that EC centrosome overduplication is linked to
226 microtubule defects, with increased nucleations and catastrophes accompanied by
227 forward-rearward polarity defects [17]. Changes in microtubule dynamics are linked to
228 regulation of adherens junctions in EC [31]. Our data indicate that adherens junctions

229 are significantly disrupted in EC with excess centrosomes, suggesting that junctions are
230 disrupted downstream of centrosome-induced microtubule defects.
231
232 Lumen structure is also disrupted downstream of excess centrosomes in
233 sprouting EC, suggesting an apical-basal polarity defect. It is likely that junctional
234 defects contribute to poor lumenization *in vitro* and *in vivo*. VE-cadherin at EC junctions
235 is linked to vascular lumen formation during anastomosis [32,33]. Moreover, genetic
236 loss of VE-cadherin in mice or zebrafish leads to lumen defects, vascular dysfunction,
237 and embryonic lethality [22,23], supporting a link between disrupted adherens junctions
238 and malformed lumens in EC sprouts. Proper adherens junctions are necessary to
239 stabilize tight junctions and form lumens [34,35] , and here we show that tight junction
240 formation is also compromised in EC with excess centrosomes, suggesting that tight
241 junction defects contribute to lumen defects.
242
243 We show that lumens are perturbed following centrosome overduplication in both
244 an *in vitro* angiogenesis model lacking physiological flow and *in vivo*, in zebrafish with
245 blood flow. These findings indicate that the lumenal defects resulting from excess
246 centrosomes do not depend on shear stress exerted by blood flow. While lumenization
247 requires blood flow during late stages of angiogenesis [36], lumens also form *in vitro*
248 and *in vivo* absent blood flow [7,37]. Disruption of the VE-cadherin junctional complex is
249 sufficient to prevent luminal expansion independent of blood flow through changes in
250 cell contractility [37]; thus, it is likely that the profound changes in VE-cadherin
251 localization at EC cell-cell junctions following centrosome over-duplication alter the

252 ability of EC to properly coordinate the cytoskeletal forces needed for polarization and
253 lumenogenesis.
254
255 Centrosome amplification is a common phenomenon in tumors and has been
256 linked to changes in the tumor microenvironment, including endothelial cells [13,14].
257 Local hypoxia in tumors increases VEGF-A signaling, leading to high CyclinE/cdk2 that
258 promotes EC centrosome overduplication [19], and elevated *Plk4* expression occurs in
259 human and mouse tumor vessels [38,39]. Although therapies targeting angiogenesis
260 have had mixed results [40,41], understanding tumor EC responses is necessary for
261 design of more complex multi-modal anti-tumor therapies [41–44]. In summary, by
262 revealing a unique link between centrosome perturbation and adherens junction stability
263 and lumenization, our data indicate a novel role for the centrosome in EC polarity,
264 junctions, and lumenization in blood vessels. These abnormalities may contribute to
265 tumor blood vessel dysfunction.

266 **MATERIALS & METHODS**

267 ***Cell culture***

268 HUVEC (C2519A, lot 486264, Lonza) were cultured in EBM-2 (CC-3162, Lonza)
269 supplemented with the Endothelial Growth Medium (EGM-2) bullet kit (CC-3162, Lonza)
270 and 1x antibiotic-antimycotic (Gibco). Normal human lung fibroblasts (CC2512, Lonza)
271 were cultured in DMEM (Gibco) with 10% fetal bovine serum (FBS) and 1x antibiotic-
272 antimycotic (Gibco). All cells were maintained at 37°C and 5% CO_2. Tetracycline-
273 inducible Plk4-overexpression HUVEC were generated as previously described
274 [13,17,25]. Viruses were produced by the UNC Lenti-shRNA Core Facility. To induce
275 centrosome overduplication, tet-Plk4 HUVEC were treated with 1µg/ml doxycycline
276 (DOX, D9891, Sigma) for 24hr followed by washout. Experiments were performed 48hr
277 following DOX addition.

278

279 ***3D sprouting angiogenesis assay***

280 The 3D sprouting angiogenesis assay was performed as previously described
281 with the following changes [17,45]. Tet-Plk4 HUVEC were treated with 1µg/ml DOX for
282 24hr at 37°C. 13µl/ml centrin:eGFP lentivirus and 1µg/ml Polybrene were added to
283 HUVEC 16hr post DOX addition for the last 8hr of DOX treatment. Cells were washed
284 with Dulbecco's phosphate-buffered saline (DPBS) (MT-21-031-CV, Corning) and fresh
285 media was added. The following day, infected cells were coated onto cytodex 3
286 microcarrier beads (17048501, GE Healthcare Life Sciences) and embedded in a fibrin
287 matrix as described. Z-stacks were acquired with an Olympus confocal microscope
288 (FV1200 or FV3000) and processed in Image J (National Institutes of Health). Total

289 vessel width was measured in the YZ plane by drawing a line through the nucleus and
290 across the entire vessel. Lumen width was measured in the YZ plane using Moesin1
291 staining (1:1000, ab52490, Abcam) as a surrogate for the apical surface and normalized
292 to total vessel width. Lumens were considered “narrow” if the normalized lumen width
293 fell below the mean lumen width minus one standard deviation of the normal condition.
294 Lumens were considered “closed” if the lumen width was zero. DAPI (10236276001,
295 Sigma) was used to visualize the nucleus, and VE-cadherin was used to visualize
296 adherens junctions (1:1000, 2500S, Cell Signaling).
297
298 ***Micropatterns***
299 Large H-micropatterns (1600 μm^2, CYTOO) were coated with 5μg/ml fibronectin
300 and seeded with HUVEC according to manufacturer’s instructions. Cells were allowed
301 to spread for 24hr, then fixed with ice-cold methanol for 10 min at 4°C.
302
303 ***Immunofluorescence and quantification***
304 Fixed HUVEC were blocked for 1hr at RT in blocking solution (5% FBS, 2X
305 antibiotic-antimycotic (Gibco), 0.1% sodium azide (s2002-100G, Sigma) in DPBS). Cells
306 were incubated in primary antibody overnight at 4°C, then washed 3X for 5 min in
307 DPBS. Secondary antibody and DRAQ7 (1:1000, ab109202, Abcam) were added for
308 1hr at RT followed by 3X washes for 10 min each in DPBS. Slides were mounted with
309 coverslips using Prolong Diamond Antifade mounting medium (P36961, Life
310 Technology) and sealed with nail polish. Primary and secondary antibodies were diluted
311 in blocking solution. Images were acquired with an Olympus confocal microscope

312 (FV1200 or FV3000) and analyzed using ImageJ. Centrosome overduplication was
313 quantified by counting centrosome number in at least 500 cells per replicate. Junction
314 area on micropatterns was quantified by thresholding VE-cadherin staining and
315 measuring total area within the junction in ImageJ. VE-cadherin distribution on doublet
316 micropatterns was measured in ImageJ by drawing a line across the junction (from
317 centrosome in first cell to centrosome in second cell) and acquiring a line scan of VE-
318 cadherin intensity. Peaks were counted for each pattern and normalized to the line
319 length. Only peaks above half of the maximum VE-cadherin intensity were counted.
320 Junction width was measured by creating a histogram of the VE-cadherin signal
321 integrated over the y-axis and measuring the width of the most prominent peak(s). The
322 following primary antibodies were used: anti-γ-tubulin (1:5000, T6557, Sigma-Aldrich),
323 anti-VE-cadherin (1:500, 2500S, Cell Signaling), anti-ZO-1 (1:500, MABT339, Millipore
324 Sigma), anti-Moesin-1 (1:1000, ab52490, Abcam). The following secondary antibodies
325 from Life Technologies were used: goat anti-mouse AlexaFluor 488 (1:500, A11029),
326 goat anti-mouse AlexaFluor 594 (1:500, A11005), goat anti-mouse AlexaFluor 647
327 (1:500, A21236) goat anti-rabbit AlexaFluor 488 (1:500, A11034), goat anti-rabbit
328 AlexaFluor 594 (1:500, A11037).
329
330 ***Zebrafish***
331 Zebrafish (*Danio rerio*) were housed in an institutional animal care and use
332 committee (IACUC)-approved facility and maintained as previously described (Wiley, *et*
333 *al*., 2011). *Tg(kdrl:mCherry)* was a gift from D. Stainier. *Tg(fli:Gal4)* was a gift from W.
334 Herzog. *Tg(fli:centrin-GFP*) was created by subcloning centrin:GFP into the

335 pCR8/GW/TOPO middle entry vector (Thermo Fisher) and then gateway cloning into
336 the pDestTol2CG2 plasmid (REF Tol2 kit). Tol2 transposase RNA was generated using
337 the sp6 mMessage mMachine synthesis kit (AM1340, Thermo Fisher). For
338 overexpression of *Plk4*, *p2a-Lox-mCherry-STOP-Lox-Plk4* was fused to the 3' end of
339 the endogenous *kdrl* gene. The assembled construct was subcloned into the pKHR4
340 backbone and linearized by I-SceI digest. This construct, 200ng/µl sgRNA (5'-
341 *TCTGGTTTGGAAGGACACAG*-3'), and 700ng/µl of Cas9 recombinant protein
342 (PNABio) were injected into one-cell stage *Tg(fli:centrin-GFP)* embryos to generate
343 double stranded breaks at the 3' end of the *kdrl* gene and induce homologous
344 recombination as previous described [46]. F1 fish were injected with Cre mRNA at the
345 1-2 cell stage. Cre mRNA was obtained by subcloning the *Cre* gene from the pME-
346 ERT2-Cre-ERT2 plasmid into the pCR8/GW/TOPO middle entry vector, gateway
347 cloning into a pCS Dest vector, then preparing RNA with the sp6 mMessageMachine
348 synthesis kit. pME-ERT2-Cre-ERT2 was a gift from Kryn Stankunas (Addgene plasmid
349 # 82587; http://n2t.net/addgene:82587; RRID:Addgene 82587). Embryos were collected
350 from desired crosses and grown in E3 at 28.5°C. At 72 hpf, embryos were injected with
351 Qdot605 (Q10103MP, Thermo Fisher). *Plk4* overexpression was determined by the loss
352 of mCherry signal. A second fish model was generated as follows: a *5X-UAS-Plk4*
353 construct was generated using Gibson cloning by fusing a *5X-UAS* tag upstream of
354 zebrafish *Plk4*. pUAS:Cas9T2AGFP;U6:sgRNA1;U6:sgRNA2 was a gift from Filippo Del
355 Bene (Addgene plasmid #74009; http://n2t.net/addgene:74009;RRID:Addgene_74009)
356 [47]. This construct and I-SceI meganuclease were injected into one-cell fish from
357 crosses between Tg(fli:centrin-GFP) and Tg(fli:Gal4;kdrl:mCherry), and fish were grown

358 in E3 at 28.5°C to 72 hpf. Fish were fixed by incubating dechorionated embryos in ice
359 cold 4% PFA at 4°C overnight. Embryos were rinsed in PBS and mounted using a fine
360 probe to de-yolk and a small blade to separate the trunk from the cephalic region, and
361 mounting with VECTASHIELD® Hardset™ Antifade Mounting Medium. The coverslip
362 was sealed with petroleum jelly before imaging on an Olympus FV1200 confocal
363 microscope. Centrosome overduplication was confirmed based on centrin-GFP centriole
364 labeling. ISV perfusion was measured by counting the number of perfused ISVs based
365 on Qdot605 signal as a percentage of total ISV number (visualized using
366 *Tg(kdrl:mCherry)*). Lumen width was measured by measuring the diameter of perfused
367 ISVs near the junction with the dorsal aorta. Lumens were considered "narrow" if the
368 lumen width fell below the mean lumen width minus one standard deviation of the
369 WT+Cre condition. Lumens were considered closed if the ISV perfusion was
370 discontinuous.
371
372 ***Statistics***
373 Student's two-tailed *t* test was used to determine statistical significance in
374 experiments with 2 groups. One-way ANOVA with Tukey's multiple comparisons test
375 was used to determine statistical significance for experiments with 3 groups, and X^2 was
376 used for categorical data. Error bars represent the mean ± standard deviation. Statistical
377 tests and graphs were made using the Prism 7 software (GraphPad Software).
378
379 **ACKNOWLEGMENTS**

380 We thank Tony Perdue and the UNC Biology Microscopy Core, the UNC Lenti-
381 shRNA Core, Maryanna Parker and Kaitlyn Quigley for fish room support, and Bautch
382 lab members for critical discussions.
383
384 **FUNDING**
385 This work was supported by grants from the National Institutes of Health
386 (HL43174, HL116719, HL117256, HL139950 to VLB), a K99/R00 (1K99HL124311-
387 01A1 to EJK), the Integrated Vascular Biology Training Grant (5T32HL069768-17 to
388 DBB), and an American Heart Association Predoctoral Fellowship (19PRE34380887 to
389 DBB).
390
391 **DECLARATION OF INTERESTS:** None.
392
393

394 **REFERENCES**

395 1. Carmeliet P, Jain RK. (2011) Molecular mechanisms and clinical applications of
396 angiogenesis. Nature. 473(7347):298–307.
397 2. Bautch VL, Caron KM. (2015) Blood and lymphatic vessel formation. Cold Spring
398 Harb Perspect Biol. 7(3):a008268.
399 3. Kushner E, Bautch V. (2013) Building blood vessels in development and disease.
400 Curr Opin Hematol. 20(3):231–6.
401 4. Blum Y, Belting HG, Ellertsdottir E, Herwig L, Luders F, Affolter M. (2008)
402 Complex cell rearrangements during intersegmental vessel sprouting and vessel
403 fusion in the zebrafish embryo. Dev Biol. 316:312–22.
404 5. Iruela-Arispe ML, Davis GE. (2009) Cellular and molecular mechanisms of
405 vascular lumen formation. Dev Cell. 16(2):222–31.
406 6. Strilic B, Kucera T, Eglinger J, Hughes MR, McNagny KM, Tsukita S, et al. (2009)
407 The molecular basis of vascular lumen formation in the developing mouse aorta.
408 Dev Cell. 17(4):505–15.
409 7. Wang Y, Kaiser MS, Larson JD, Nasevicius A, Clark KJ, Wadman SA, et al.
410 (2010) Moesin1 and VE-cadherin are required in endothelial cells during in vivo
411 tubulogenesis. Development. 137(18):3119–28.
412 8. Lee CY, Bautch VL. (2011) Ups and downs of guided vessel sprouting: the role of
413 polarity. Physiology. 26(5):326–33.
414 9. Pelton JC, Wright CE, Leitges M, Bautch VL. (2014) Multiple endothelial cells
415 constitute the tip of developing blood vessels and polarize to promote lumen
416 formation. Development. 141(21):4121–6.

417 10. Aird WC. (2012) Endothelial cell heterogeneity. Cold Spring Harb Perspect Med.
418 2(1):a006429.
419 11. Hashizume H, Baluk P, Morikawa S, McLean JW, Thurston G, Roberge S, et al.
420 (2000) Openings between defective endothelial cells explain tumor vessel
421 leakiness. Am J Pathol. 156(4):1363–80.
422 12. Carmeliet P, Jain RK. (2011) Principles and mechanisms of vessel normalization
423 for cancer and other angiogenic diseases. Nat Rev Drug Discov. 10:417–27.
424 13. Kushner EJ, Ferro LS, Liu J-Y, Durrant JR, Rogers SL, Dudley AC, et al. (2014)
425 Excess centrosomes disrupt endothelial migration via centrosome scattering. J
426 Cell Biol. 206(2):257–72.
427 14. Hida K, Hida Y, Amin DN, Flint AF, Panigrahy D, Morton CC, et al. (2004) Tumor-
428 Associated Endothelial Cells with Cytogenetic Abnormalities. Cancer Res.
429 64(22):8249–55.
430 15. Kollman JM, Merdes A, Mourey L, Agard DA. (2011) Microtubule nucleations by
431 gamma-tubulin complexes. Nat Rev Mol Cell Biol. 12:709–21.
432 16. Bettencourt-Dias M, Glover DM. (2007) Centrosome biogenesis and function:
433 centrosomics brings new understanding. Nat Rev Mol Cell Biol. 8:451–63.
434 17. Kushner EJ, Ferro LS, Yu Z, Bautch VL. (2016) Excess centrosomes perturb
435 dynamic endothelial cell repolarization during blood vessel formation. Mol Biol
436 Cell. 27(12):1911–20.
437 18. Godinho SA, Picone R, Burute M, Dagher R, Su Y, Leung CT, et al. (2014)
438 Oncogene-like induction of cellular invasion from centrosome amplification.
439 Nature. 510(7503):167–71.

440 19. Taylor SM, Nevis KR, Park HL, Rogers GC, Rogers SL, Cook JG, et al. (2010)
441 Angiogenic factor signaling regulates centrosome duplication in endothelial cells
442 of developing blood vessels. Blood. 116(16):3108–17.
443 20. Spracklen AJ, Peifer M. (2015) Actin and apical constriction: some (re)-assembly
444 required. Dev Cell. 35(6):662–4.
445 21. Nowotarski SH, Peifer M. (2014) Cell biology: a tense but good day for actin at
446 cell-cell junctions. Curr Biol. 24(15):R688–90.
447 22. Carmeliet P, Lampugnani M-G, Moons L, Breviario F, Compernolle V, Bono F, et
448 al. (1999) Targeted deficiency or cytosolic truncation of the VE-cadherin gene in
449 mice impairs VEGF-mediated endothelial survival and angiogenesis. Cell.
450 98(2):147–57.
451 23. Montero-Balaguer M, Swirsding K, Orsenigo F, Cotelli F, Mione M, Dejana E.
452 (2009) Stable vascular connections and remodeling require full expression of VE-
453 cadherin in zebrafish embryos. PLoS One. 4(6):e5772.
454 24. Habedanck R, Stierhof YD, Wilkinson CJ, Nigg EA. (2005) The Polo kinase Plk4
455 functions in centriole duplication. Nat Cell Biol. 7(11):1140–6.
456 25. Yu Z, Ruter DL, Kushner EJ, Bautch VL. (2017) Excess centrosomes induce p53-
457 dependent senescence without DNA damage in endothelial cells. FASEB J.
458 10:4295–304.
459 26. Iden S, Rehder D, August B, Suzuki A, Wolburg-Buchholz K, Wolburg H, et al.
460 (2006) A distinct PAR complex associates physically with VE-cadherin in
461 vertebrate endothelial cells. EMBO Rep. 7(12):1239–46.
462 27. Bentley K, Franco CA, Philippides A, Blanco R, Dierkes M, Gebala V, et al. (2014)

463 The role of differential VE-cadherin dynamics in cell rearrangement during
464 angiogenesis. Nat Cell Biol. 16(4):309–21.
465 28. Paatero I, Sauteur L, Lee M, Lagendijk AK, Heutschi D, Wiesner C, et al. (2018)
466 Junction-based lamellipodia drive endothelial cell rearrangements in vivo via a
467 VE-cadherin-F-actin based oscillatory cell-cell interaction. Nat Commun.
468 9(1):3545.
469 29. Lampugnani M-G, Orsenigo F, Rudini N, Maddaluno L, Boulday G, Chapon F, et
470 al. (2010) CCM1 regulates vascular-lumen organization by inducing endothelial
471 polarity. J Cell Sci. 123:1073–80.
472 30. Mikule K, Delaval B, Kaldis P, Jurcyzk A, Hergert P, Doxsey S. (2007) Loss of
473 centrosome integrity induces p38-p53-p21-dependent G1-S arrest. Nat Cell Biol.
474 9:160–70.
475 31. Komarova YA, Huang F, Geyer M, Daneshjou N, Garcia A, Idalino L, et al. (2012)
476 VE-cadherin signaling induces EB3 phosphorylation to suppress microtubule
477 growth and assemble adherens junctions. Mol Cell. 48(6):914–25.
478 32. Lenard A, Ellertsdottir E, Herwig L, Krudewig A, Sauteur L, Belting H-G, et al.
479 (2013) In vivo analysis reveals a highly stereotypic morphogenetic pathway of
480 vascular anastomosis. Dev Cell. 25(5):492–506.
481 33. Herwig L, Blum Y, Krudewig A, Ellertsdottir E, Lenard A, Belting H-G, et al. (2011)
482 Distinct cellular mechanisms of blood vessel fusion in the zebrafish embryo. Curr
483 Biol. 21(22):1942–8.
484 34. Campbell HK, Maiers JL, DeMali KA. (2017) Interplay between tight junctions and
485 adherens junctions. Exp Cell Res. 358(1):39–44.

486 35. Odenwald MA, Choi W, Buckley A, Shashikanth N, Joseph NE, Wang Y, et al.
487 (2017) ZO-1 interactions with F-actin and occludin direct epithelial polarization
488 and single lumen specification in 3D culture. J Cell Sci. 130(1):243–59.
489 36. Gebala V, Collins R, Geudens I, Phng L-K, Gerhardt H. (2016) Blood flow drives
490 lumen formation by inverse membrane blebbing during angiogenesis in vivo. Nat
491 Cell Biol. 18(4):443–50.
492 37. Hultin S, Zheng Y, Mahdi M, Vertuani S, Gentili C, Balland M, et al. (2014)
493 AmotL2 links VE-cadherin to contractile actin fibres necessary for aortic lumen
494 expansion. Nat Commun. 5:3743.
495 38. Roudnicky F, Poyet C, Wild P, Krampitz S, Negrini F, Huggenberger R, et al.
496 (2013) Endocan is upregulated on tumor vessels in invasive bladder cancer
497 where it mediates VEGF-A-induced angiogenesis. Cancer Res. 73(3):1097–106.
498 39. Goveia J, Rohlenova K, Taverna F, Treps L, Conradi L, Pircher A, et al. (2020) An
499 integrated gene expression landscape profiling approach to identify lung tumor
500 endothelial cell heterogeneity and angiogenic candidates. Cancer Cell. 37(1):21–
501 36.
502 40. Brossa A, Buono L, Fallo S, Pla AF, Munaron L, Bussolati B. (2019) Alternative
503 strategies to inhibit tumor vascularization. Int J Mol Sci. 20:6180.
504 41. Tamura R, Tanaka T, Akasaki Y, Murayama Y, Yoshida K, Sasaki H. (2019) The
505 role of vascular endothelial growth factor in the hypoxic and immunosuppressive
506 tumor microenvironmnet: perspectives for therapeutic implications. Med Oncol.
507 37(2).
508 42. Sakurai Y, Akita H, Harashima H. (2019) Targeting tumor endothelial cells with

509 nanoparticles. Internaltional J Mol Sci. 20(23):5819.

510 43. Zhao Y, Wang X. (2019) Plk4: a promising target for cancer therapy. J Cancer
511 Res Clin Oncol. 145:2413–22.

512 44. Rivera-Rivera Y, Saavedra HI. (2016) Centrosome - a promising anti-cancer
513 target. Biologics. 10:167–76.

514 45. Nakatsu MN, Hughes CCW. (2008) An optimized three-dimensional in vitro model
515 for the analysis of angiogenesis. Methods Enzymol. 443:65–82.

516 46. Hoshijima K, Jurynec MJ, Grunwald DJ. (2016) Precise editing of the zebrafish
517 genome made simple and efficient. Dev Cell. 36(6):654–67.

518 47. Di Donato V, De Santis F, Auer TO, Testa N, Sánchez-Iranzo H, Mercader N, et
519 al. (2016) 2C-Cas9: a versatile tool for clonal analysis of gene function. Genome
520 Res. 26(5):681–92.

521

522 **FIGURE LEGENDS**

523 **Figure 1. Excess centrosomes perturb polarity between EC sharing junctions.**
524 **(a)** Schematic of *Plk4* overexpression in HUVEC. TRE, tet-responsive element; rtTA,
525 reverse tet transactivator. **(b)** Schematic of H-micropattern with possible centrosome
526 positions. **(c)** Representative images of EC on H-micropatterns with either 1-2
527 centrosomes (left) or >2 centrosomes (right). Yellow arrowheads, 1-2 centrosomes with
528 distal localization; white arrowheads, >2 centrosomes with central localization;
529 centrosome (γ-tubulin, green); DNA (blue, DRAQ7). Insets, γ-tubulin. Scale bar, 10μm.
530 **(d)** Quantification of EC centrosome position based on pattern orientation and EC with
531 1-2 centrosomes (N) or >2 centrosomes (O). **(e)** Quantification of polarity based on
532 pattern orientation. **(f)** Quantification of polarity mismatch. N=4 replicates. Statistics: χ^2
533 analysis. (N:N), both EC 1-2 centrosomes/cell; (O:O), both EC >2 centrosomes/cell;
534 (N:O) one EC 1-2 centrosomes, one EC >2 centrosomes.
535

536 **Figure 2. EC with excess centrosomes form disorganized adherens junctions.**
537 **(a-a'')** Schematics showing potential arrangement of EC on H-patterns. **(b-b'')**
538 Representative images of cell-cell junctions on H patterns with EC centrosome status
539 N:N **(b)**, N:O **(b')**, or O:O **(b'')**. EC were stained for γ-tubulin (green, centrosome), VE-
540 cadherin (red, junctions), and DRAQ7 (blue, DNA). Scale bar, 10μm. **(c-c'')**
541 Representative VE-cadherin line scans between centrosomes in N:N **(c)**, N:O **(c')**, or
542 O:O **(c'')** EC junctions. #, positive peak. **(d)** Quantification of VE-cadherin area in EC
543 junctions with the indicated centrosome complements. **(e)** Quantification of peaks/length
544 of VE-cadherin line scans of EC junctions with indicated centrosome complements. **(f)**

545 Quantification of junction width of EC with indicated centrosome complements. N=4
546 replicates. Statistics: one-way ANOVA with Tukey's correction. *, $p \leq 0.05$, **, $p \leq 0.01$, ***,
547 $p \leq 0.001$, ****, $p \leq 0.0001$.
548
549 **Figure 3. Sprouts containing EC with excess centrosomes have abnormal**
550 **lumens.**
551 **(a)** Schematic showing the XY plane of vessel sprout and centrosome position scoring
552 criteria. **(b)** Representative images showing lumen diameter in EC with indicated
553 centrosome number. Left panels, XY axis; right panels, YZ axis. Centrin::GFP (green,
554 centrosome), Moesin1 (red, apical), DNA (cyan, DAPI). Insets, centrin-GFP. Scale bar,
555 10µm. **(c)** Apical-basal centrosome position in sprouting EC with indicated centrosome
556 number. N=3 replicates. Statistics: χ^2 analysis. **(d)** Moesin1 staining pattern in EC with
557 indicated centrosome numbers. N=3 replicates. Statistics: χ^2 analysis. **(e)** Quantification
558 of lumen diameter in EC with indicated centrosome number. N=3 replicates. Statistics:
559 one-way ANOVA with Tukey's correction. **, $p \leq 0.01$. **(f)** Quantification of open, narrow,
560 or closed lumens in EC with indicated centrosome number. N=3 replicates. Statistics: χ^2
561 analysis.
562
563 **Figure 4. *Plk4* overexpression in zebrafish results in fewer lumenized vessels.**
564 **(a-a'')** Representative images of zebrafish tails at 72 hpf perfused with Qdot605 to
565 assess lumen formation in embryos of indicated genotype and indicated injection with
566 Cre. Blue arrowheads, open lumens; red arrowheads, narrow lumens; green
567 arrowheads, closed lumens. Insets, examples of different lumen categories. LSL, lox-

568 STOP-lox. **(b)** Quantification of ISV perfusion in 72 hpf fish with indicated
569 gentoypes/condition (WT + Cre, n=5 fish; LSL-Plk4 uninjected, n=31; LSL-Plk4 + Cre,
570 n=28). **(c)** Quantification of lumen width in 72 hpf fish with indicated genotypes/condition
571 (WT + Cre, n=86 lumens; LSL-Plk4 uninjected, n=628; LSL-Plk4 + Cre, n=450).
572 Statistics: one-way ANOVA with Tukey's correction. *, $p \leq 0.05$, ****, $p \leq 0.0001$. **(d)**
573 Quantification of open, narrow, or closed lumens in vessels of 72 hpf fish with indicated
574 genotypes/condition. N=5 fish/condition. Statistics: χ^2 analysis. **(e)** Representative
575 images of ISVs from 72 hpf embryos characterized by presence of *Tg(fli:Gal4)* and
576 centrosome number. *Tg(kdrl:mCherry)* (red), *Tg(fli:centrin-GFP)* (green). Insets, centrin-
577 GFP. Scale bar, 20μm. **(f)** Quantification of ISV width with indicated genotypes/condition
578 (Fli:Gal4 negative, n=4 fish; Fli:Gal4 positive, n=13). Statistics: one-way ANOVA with
579 Tukey's correction.
580
581
582

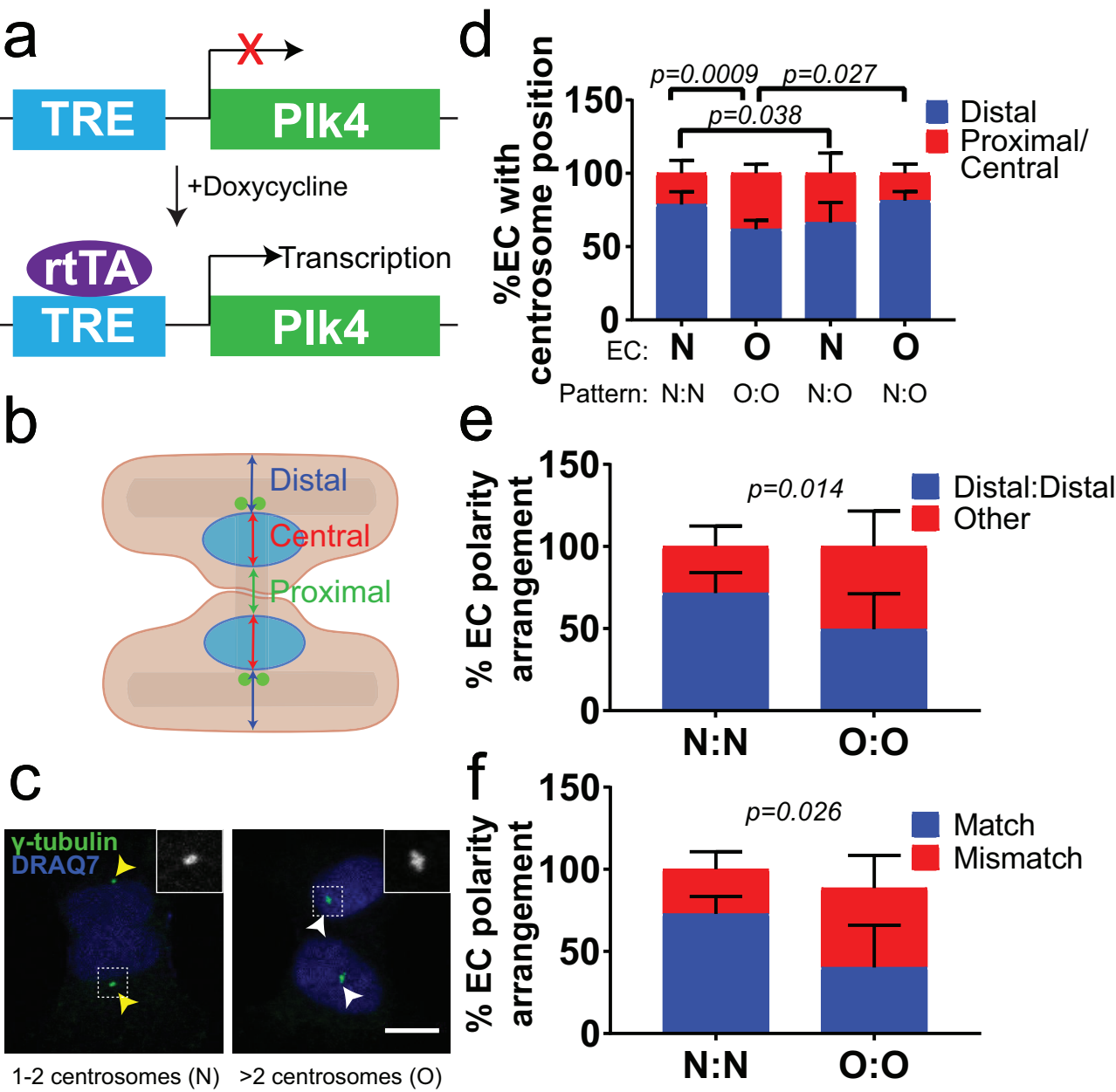
a
TRE
Plk4
+Doxycycline
rtTA
TRE
Transcription
Plk4
b
Distal
Central
Proximal
c
γ-tubulin
DRAQ7
1-2 centrosomes (N)
>2 centrosomes (O)
d
%EC with centrosome position
p=0.0009
p=0.027
p=0.038
Distal
Proximal/ Central
EC: N O N O
Pattern: N:N O:O N:O N:O
e
% EC polarity arrangement
p=0.014
Distal:Distal
Other
N:N
O:O
f
% EC polarity arrangement
p=0.026
Match
Mismatch
N:N
O:O

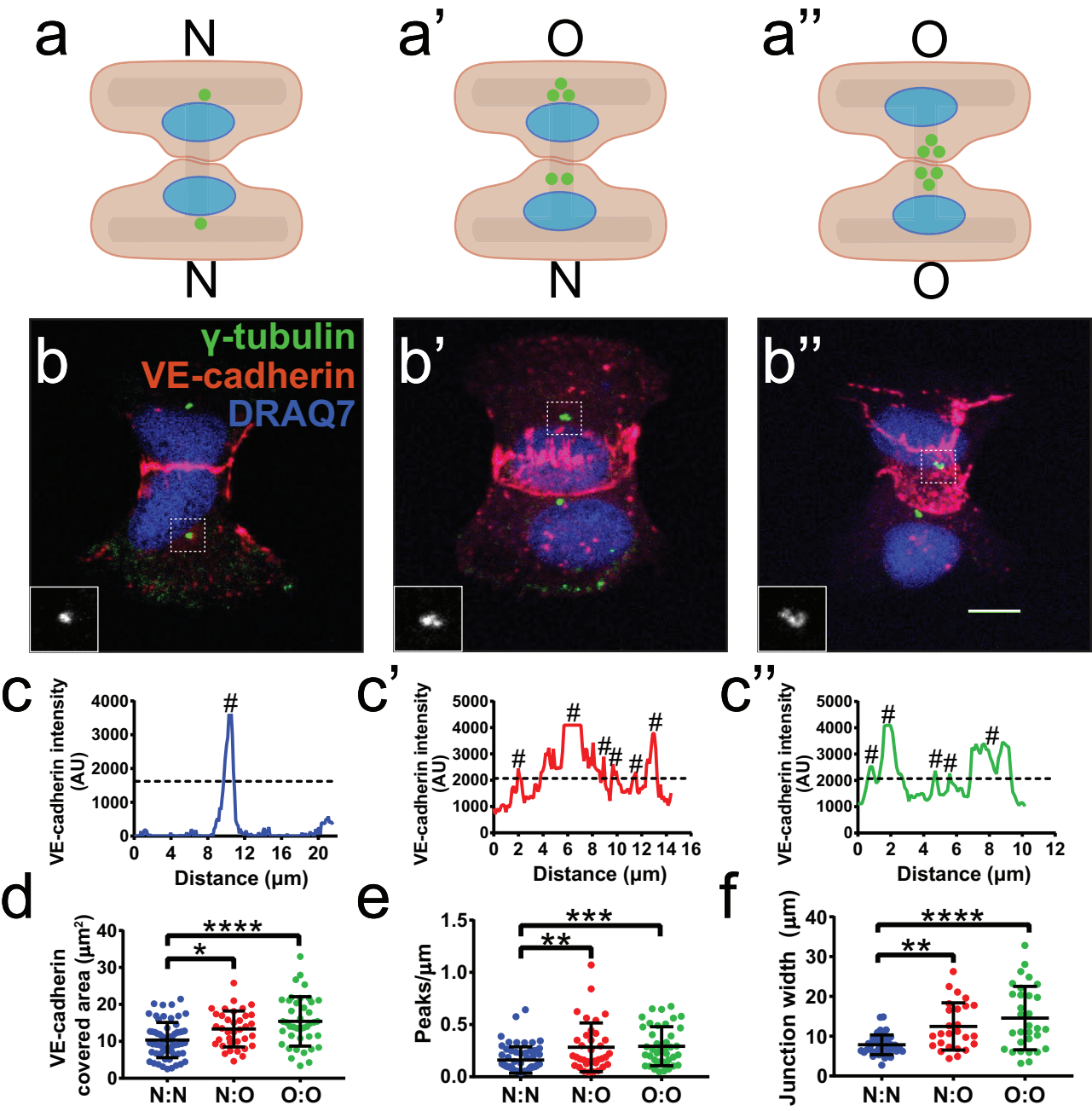
a
N
N
a'
O
N
a''
O
O
b
γ-tubulin
VE-cadherin
DRAQ7
b'
b''
c
VE-cadherin intensity (AU)
Distance (μm)
c'
c''
d
VE-cadherin covered area (μm²)
N:N
N:O
O:O
e
Peaks/μm
f
Junction width (μm)

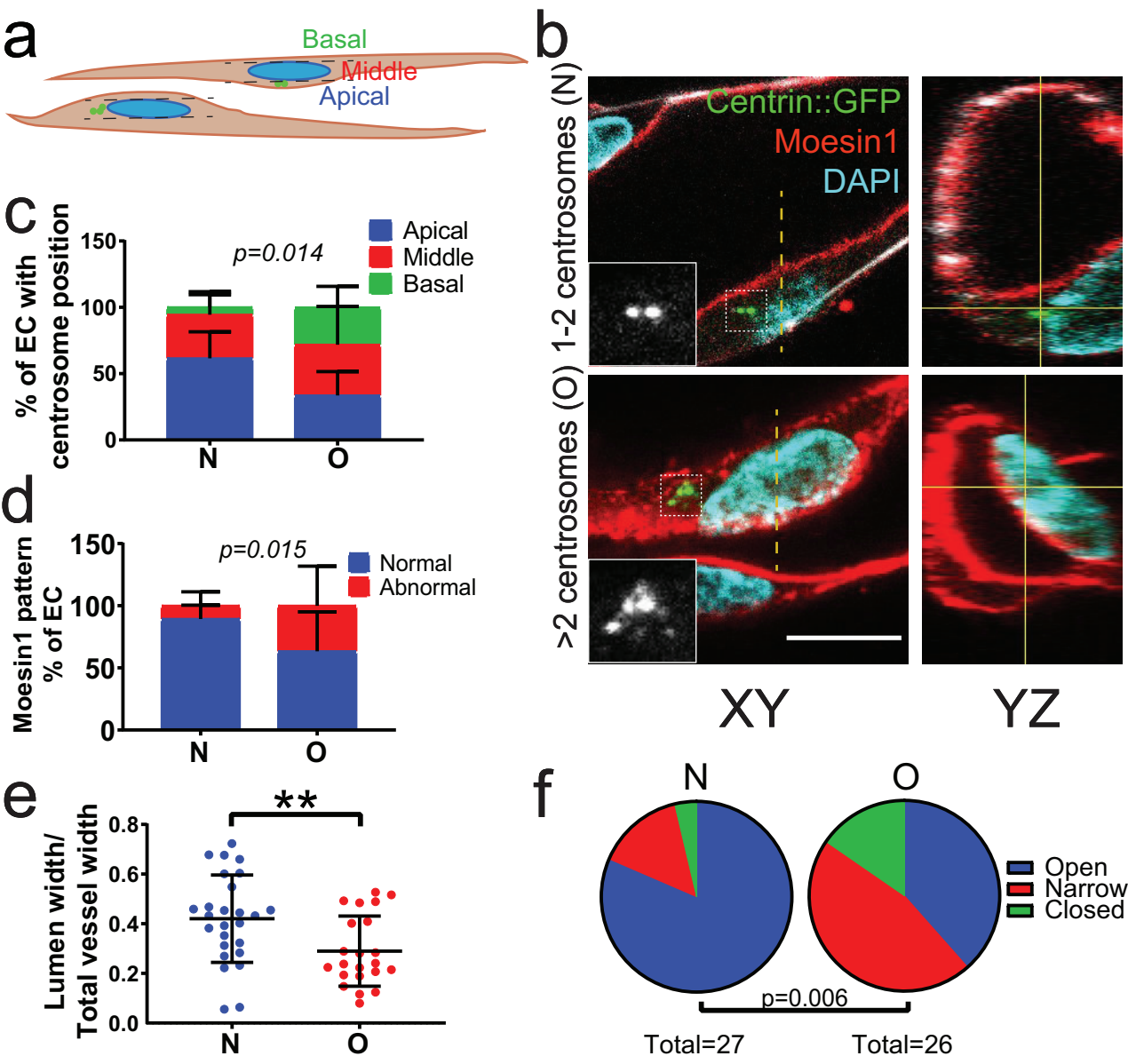
a
Basal
Middle
Apical
b
Centrin::GFP
Moesin1
DAPI
1-2 centrosomes (N)
>2 centrosomes (O)
XY
YZ
c
% of EC with centrosome position
p=0.014
Apical
Middle
Basal
150
100
50
0
N
O
d
Moesin1 pattern % of EC
p=0.015
Normal
Abnormal
150
100
50
0
N
O
e
Lumen width/ Total vessel width
**
0.8
0.6
0.4
0.2
0.0
N
O
f
N
O
Open
Narrow
Closed
p=0.006
Total=27
Total=26

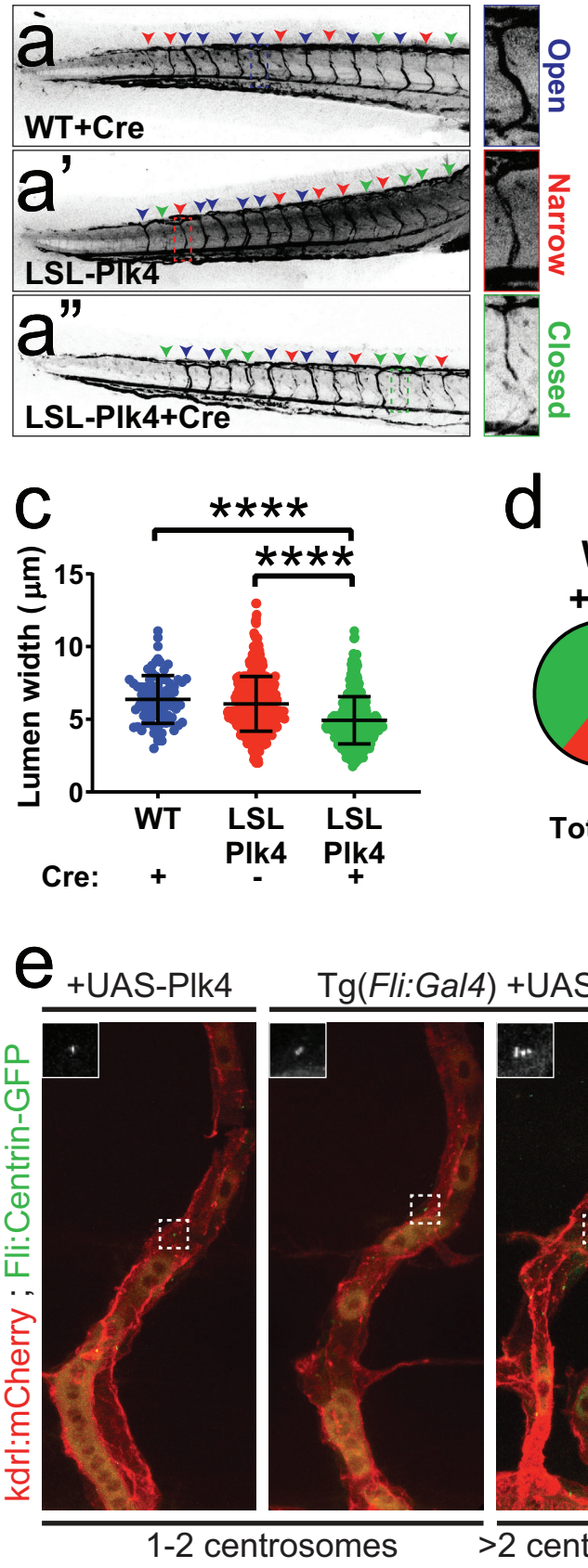
a
WT+Cre
a'
LSL-Plk4
a''
LSL-Plk4+Cre
Open
Narrow
Closed
b
% ISVs Perfused
125
100
75
50
25
0
*
****
WT
LSL Plk4
LSL Plk4
Cre: + - +
c
Lumen width (µm)
15
10
5
0
****
****
WT
LSL Plk4
LSL Plk4
Cre: + - +
d
WT +Cre
LSL-Plk4
LSL-Plk4 +Cre
Open
Narrow
Closed
p=0.012
Total=87
Total=82
Total=70
e
+UAS-Plk4
Tg(Fli:Gal4) +UAS-Plk4
kdrl:mCherry ; Fli:Centrin-GFP
1-2 centrosomes
>2 centrosomes
f
ISV width (µm)
15
10
5
0
****
****
N
N
O
Fli:Gal4 - + +

SUPPLEMENTARY MATERIAL

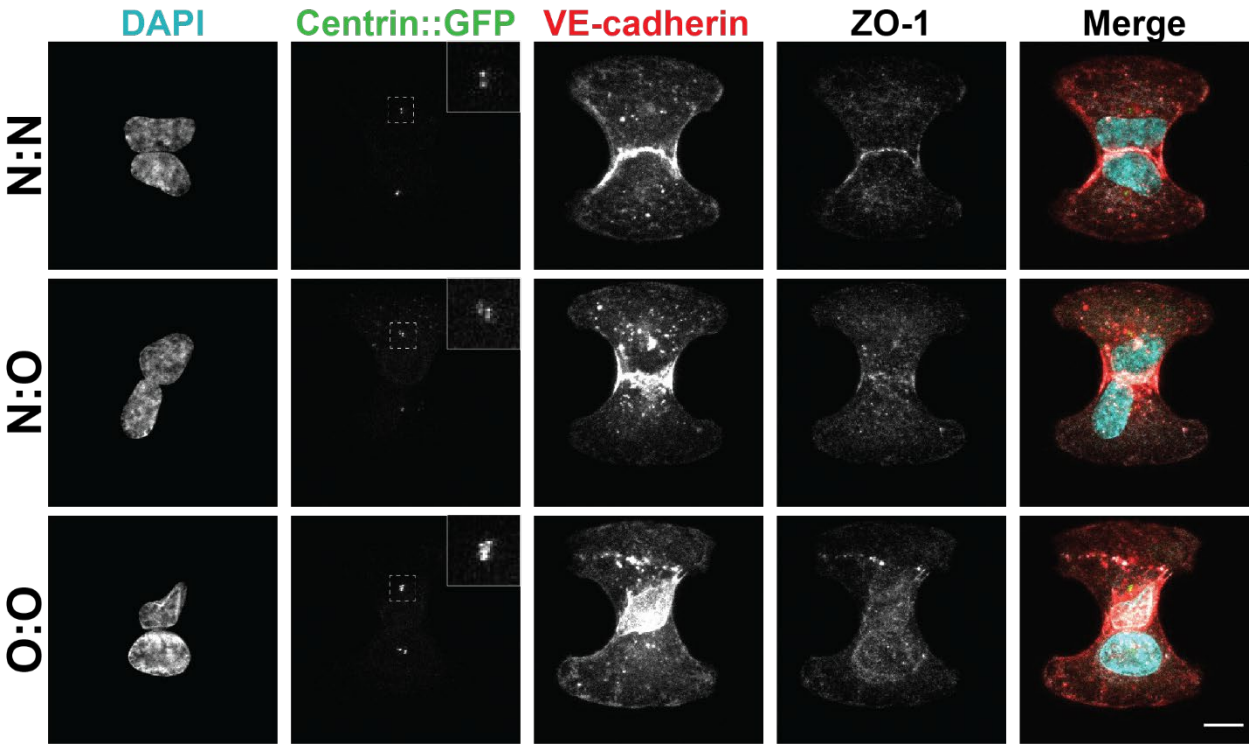

Supplementary Figure 1. EC with excess centrosomes do not form proper tight junctions.

Representative images of micropatterns with N:N, N:O, or O:O configurations. EC were labeled for DNA (cyan, DAPI), centrosomes (green, centrin::GFP), adherens junctions (VE-cadherin, red), and tight juntions (ZO-1, gray). Insets, centrin-GFP. Scale bar, 10μm.

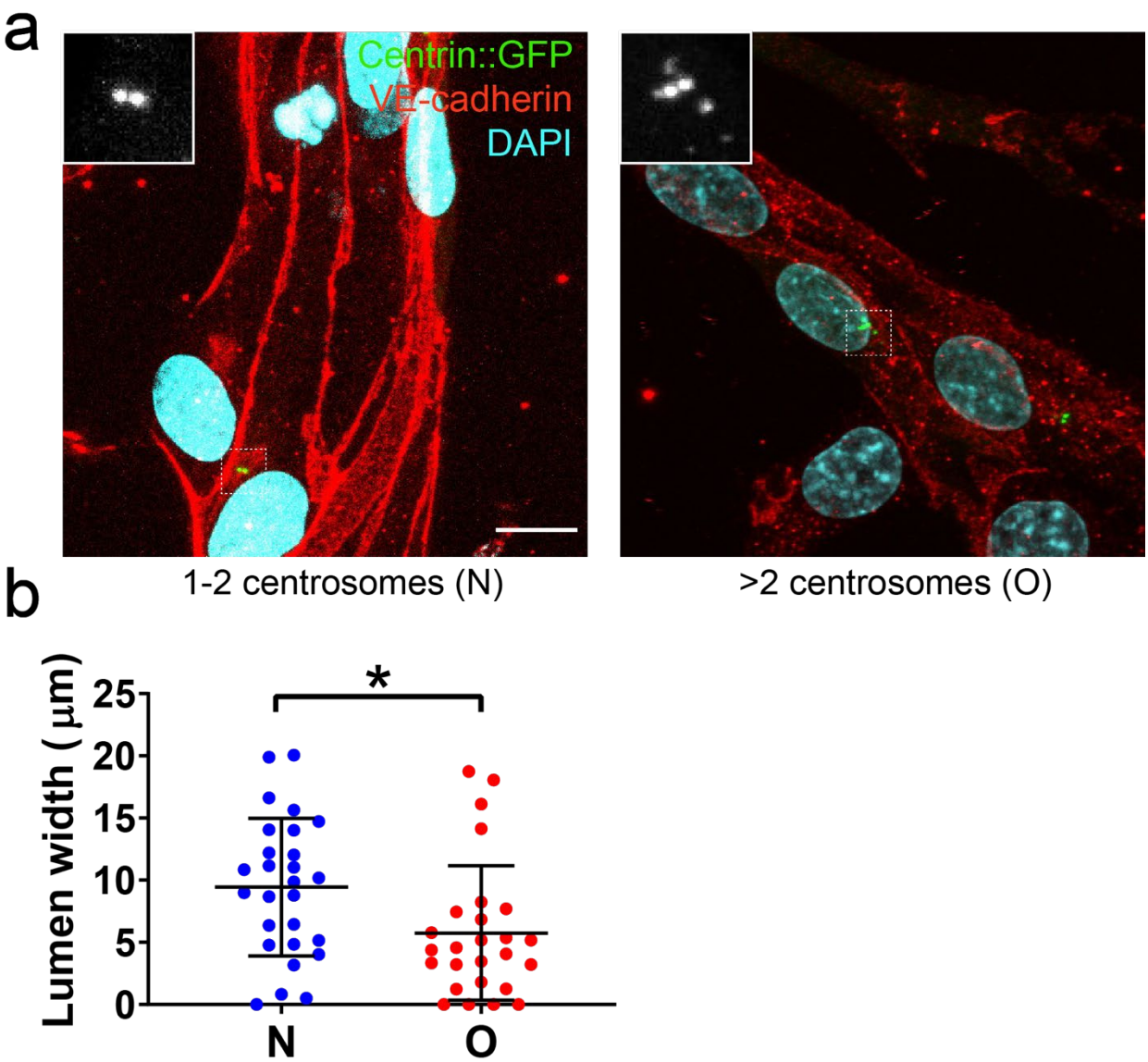

Supplementary Figure 2. EC with excess centrosomes have disrupted junctions and lumens in 3D sprouts.

(a) Representative images of 3D sprouts showing junctions in EC with indicated centrosome number. EC are labeled for DNA (cyan, DAPI), centrosomes (green, centrin::GFP), and adherens junctions (VE-cadherin, red). Insets, centrin-GFP. Scale bar, 10 µm. **(b)** Quantification of raw lumen width (not normalized to vessel width). n=3 replicates. Statistics: one-way ANOVA with Tukey's correction.

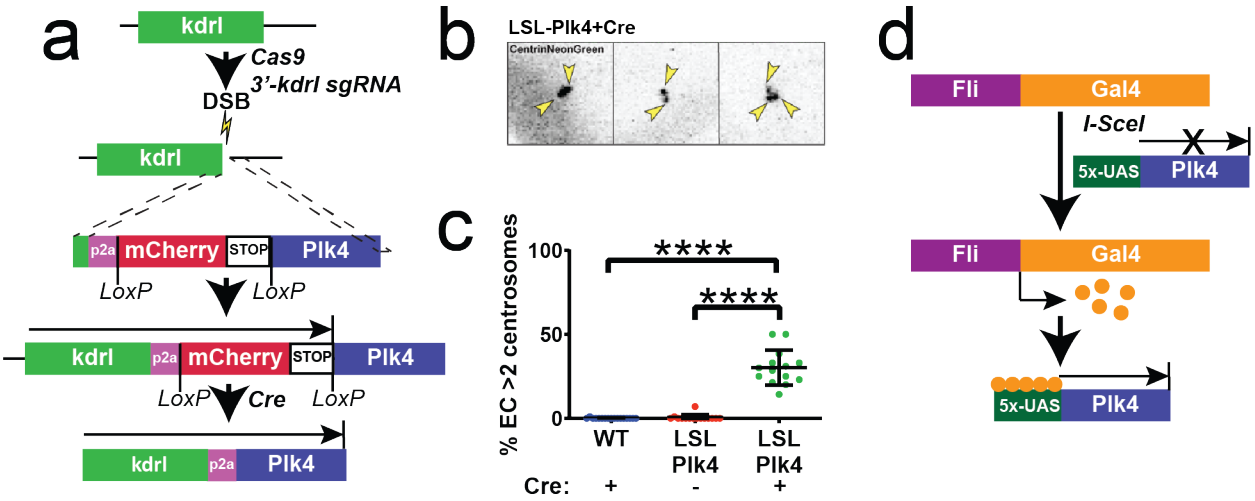

Supplementary Figure 3. *Plk4* overexpression in zebrafish leads to excess centrosomes.

(a) Schematic for Cre-mediated *Plk4* overexpression in zebrafish. **(b)** Representative image of *Plk4* overexpression in 72 hpf zebrafish. Yellow arrowheads, EC centrosome number. **(c)** Quantification of EC with >2 centrosomes in zebrafish with indicated genotypes/conditions (WT + Cre, n=17 fish; LSL-Plk4 uninjected, n=15; LSL-Plk4 + Cre, n=14). Statistics: one-way ANOVA with Tukey's correction. ****, $p \leq 0.0001$. **(d)** Schematic for transient *Gal4-UAS* mediated overexpression of *Plk4* in zebrafish.